APPLIED PHYSICS LETTERS 104, 071902 (2014)

Evidence of the metal-insulator transition in ultrathin unstrained V_2O_3 thin films

L. Dillemans,[a] T. Smets, R. R. Lieten, M. Menghini, C.-Y. Su, and J.-P. Locquet
Departement Natuurkunde en Sterrenkunde, Katholieke Universiteit Leuven, Celestijnenlaan 200D, 3001 Heverlee, Belgium

(Received 13 November 2013; accepted 3 February 2014; published online 18 February 2014)

We report the strain state and transport properties of V_2O_3 layers and V_2O_3/Cr_2O_3 bilayers deposited by molecular beam epitaxy on (0001)-Al_2O_3. By changing the layer on top of which V_2O_3 is grown, we change the lattice parameters of ultrathin V_2O_3 films significantly. We find that the metal-insulator transition is strongly attenuated in ultrathin V_2O_3 layers grown coherently on Al_2O_3. This is in contrast with ultrathin V_2O_3 layers grown on Cr_2O_3 buffer layers, where the metal-insulator transition is preserved. Our results provide evidence that the existence of the transition in ultrathin films is closely linked with the lattice deformation. © *2014 AIP Publishing LLC*. [http://dx.doi.org/10.1063/1.4866004]

Vanadium sesquioxide (V_2O_3) has been the focus of intense research by both theorists and experimentalists since the discovery of a Metal-Insulator transition (MIT) in this material.[1] A phase diagram for bulk V_2O_3 was established by McWhan *et al*.[2] At ambient conditions, stoichiometric V_2O_3 is a paramagnetic metal (PM) with a rhombohedral structure that is isostructural with corundum Al_2O_3 (spacegroup R-3c). Upon cooling below 150–160 K, V_2O_3 undergoes a MIT with an increase in resistivity of over 7 orders of magnitude to an antiferromagnetic insulating state (AFI), accompanied by a monoclinic distortion. The state of the material can be influenced by stoichiometry, doping or hydrostatic pressure. These parameters have an "equivalent" effect: A "negative" pressure[3] or doping with a small percentage of Cr stabilizes a paramagnetic insulating phase that is isostructural with respect to the PM phase. On the other hand, application of hydrostatic pressure, a small percentage of Ti doping or an oxygen excess[4] results in a gradual decrease of the PM-AFI transition temperature down to 0 K, stabilizing the PM phase at all temperatures.

Thin films of materials that exhibit a MIT offer interesting prospects for integration in device structures, including piezoelectronic[5] and field-effect transistors.[6] The performance of these devices benefits in many cases from the active material being (ultra-)thin since this allows increased switching speed. Additionally, a more pronounced switching effect is expected when the active layer has a thickness comparable with the screening length ($\sim$1 nm). V_2O_3, considered to be a prototypical Mott-Hubbard system, can be used as a model system to study the MIT characteristics upon scaling. In particular, it remains an open question whether or not a pronounced MIT can be achieved in V_2O_3 ultrathin layers. The proximity of surfaces and interfaces can possibly have a dramatic effect on the transport properties. In particular, Borghi *et al*.[7] predict a surface dead layer where the quasi-particle weight at the Fermi level is reduced with respect to the bulk value for a Mott material near an interface. Evidence for the existence of such a layer has indeed been found in photoemission spectroscopy measurements of bulk V_2O_3.[8,9] Based on assumptions for the value of the photoelectron mean free path and the profile of the quasi-particle weight, Rodolakis *et al*.[9] made a rough estimate of 4 nm for the thickness of this layer. Furthermore, a number of authors report the absence or a significant attenuation of the MIT in ultrathin layers.[10–12]

In this work, we investigate the influence of a Cr_2O_3 buffer layer and the V_2O_3 thickness on the transport properties. We demonstrate a MIT in ultrathin V_2O_3 layers down to 3.5 ± 1 nm by inserting high quality and (almost) relaxed Cr_2O_3 buffer layers between the V_2O_3 and the (0001)-Al_2O_3 substrate.

Layers of V_2O_3 and Cr_2O_3 were deposited by means of oxygen assisted molecular beam epitaxy in a vacuum chamber (Riber) with a base pressure of 10^{-9} millibars. Substrates of (0001)-Al_2O_3 (1×1 cm^2) were used without prior cleaning or flash annealing at elevated temperatures. The substrates were heated slowly to the growth temperature, measured by a thermo-couple. Cr was evaporated from a Knudsen cell and V was evaporated from an electron gun (MBE Komponenten). A deposition rate of 0.1 Å/s was used for both metals. In the case of the V_2O_3/Cr_2O_3 bilayers, V_2O_3 was deposited *in-situ* right after Cr_2O_3. An oxygen partial pressure of 6×10^{-6} (2×10^{-6}) Torr and growth temperature of 700 (720) °C was used for deposition of the V_2O_3 (Cr_2O_3) layers. After deposition, the samples were characterized by means of high resolution X-ray diffraction (XRD), X-ray reflectivity (XRR), and X-ray reciprocal space mapping (RSM) using a Panalytical X'pert Pro diffractometer. Temperature dependent transport properties were assessed by performing resistivity measurements in the Van der Pauw (VDP) and collinear configurations, using Au/Cr contacts and an Oxford Optistat CF2-V cryostat with a sweep rate of 1.5 K per minute.

First, we investigated V_2O_3 layers deposited directly on (0001)-Al_2O_3. An XRD $\theta/2\theta$ scan of the (0006) reflection of a 57 nm V_2O_3 layer grown on Al_2O_3 is shown in Fig. 1. High quality epitaxial deposition with a smooth surface and interface is evident from the appearance of Pendelössung fringes. Moreover, identical thickness values are extracted from fittings of the XRR and XRD data.

[a]leander.dillemans@gmail.com

 © 2014 AIP Publishing LLC

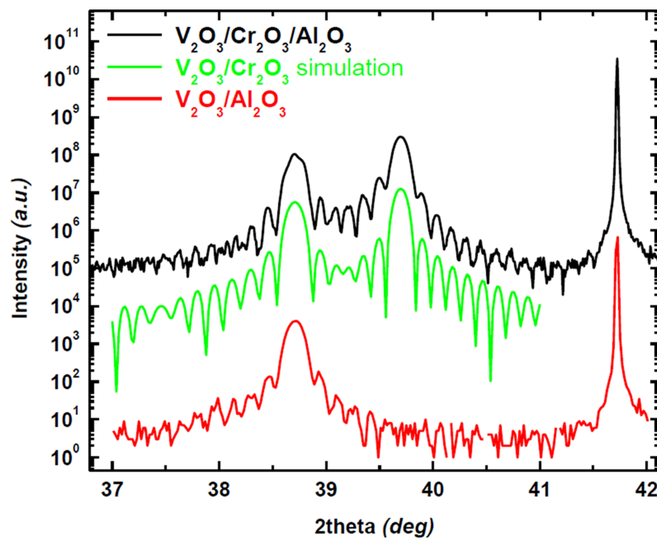

FIG. 1. XRD $\theta/2\theta$ scans for a 57 and 56 nm V_2O_3 layer grown on Al_2O_3 (red) and Cr_2O_3/Al_2O_3 (black), respectively. The green curve is a simulation of the latter.

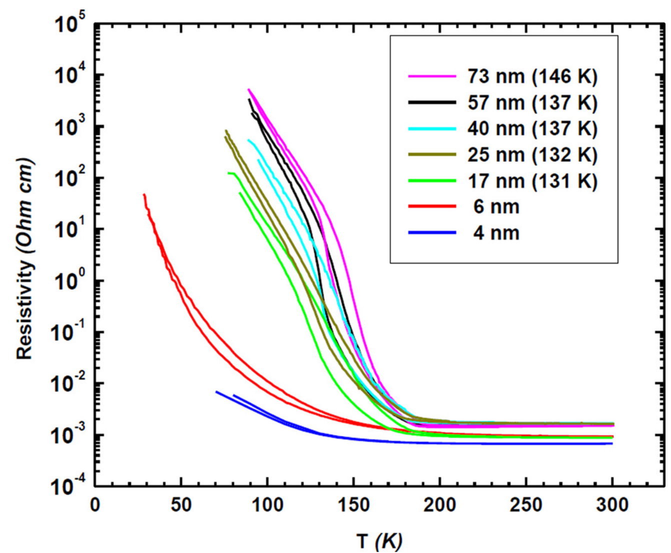

FIG. 3. Resistivity of V_2O_3 layers with different thickness deposited directly on (0001)-Al_2O_3. T_{MIT} values are given in the legend.

RSMs around the $(1\ 0\ \bar{1}\,10)$ reflections of V_2O_3 and Al_2O_3 are shown in Fig. 2 for layers with different thicknesses. The lattice parameters extracted from the peak maximum for layers with thicknesses between 73 and 17 nm (not all shown) correspond well with the bulk values of $a = 4.954$ Å and $c = 14.008$ Å, apart from a small tensile (compressive) in-plane (out-of-plane) strain scattered between 0.2 (−0.44)% and 0.34 (−0.49)%, which is most likely thermal in nature.[13] These layers exhibit elliptical peak shapes that are broadened as a result of tilt and finite in- and out-of-plane coherence lengths. In addition to a relaxed feature, the film with 17 nm thickness exhibits a faint thin stripe located at the same a-axis position as the substrate and smeared out along the c-axis direction. This is indicative of a coherent component present in the layer, lattice matched with the substrate (same Q_x). The relative intensity of the coherent feature increases systematically as the thickness is decreased to 6 and 4 nm. In the 4 nm layer, the relaxed feature is barely visible and we can conclude that the layer is almost fully coherently strained.

Resistivity hysteresis curves as a function of temperature are shown in Fig. 3 for V_2O_3 layers with different thickness grown directly on Al_2O_3. The transition temperature (T_{MIT}) is determined from the first derivative of either the

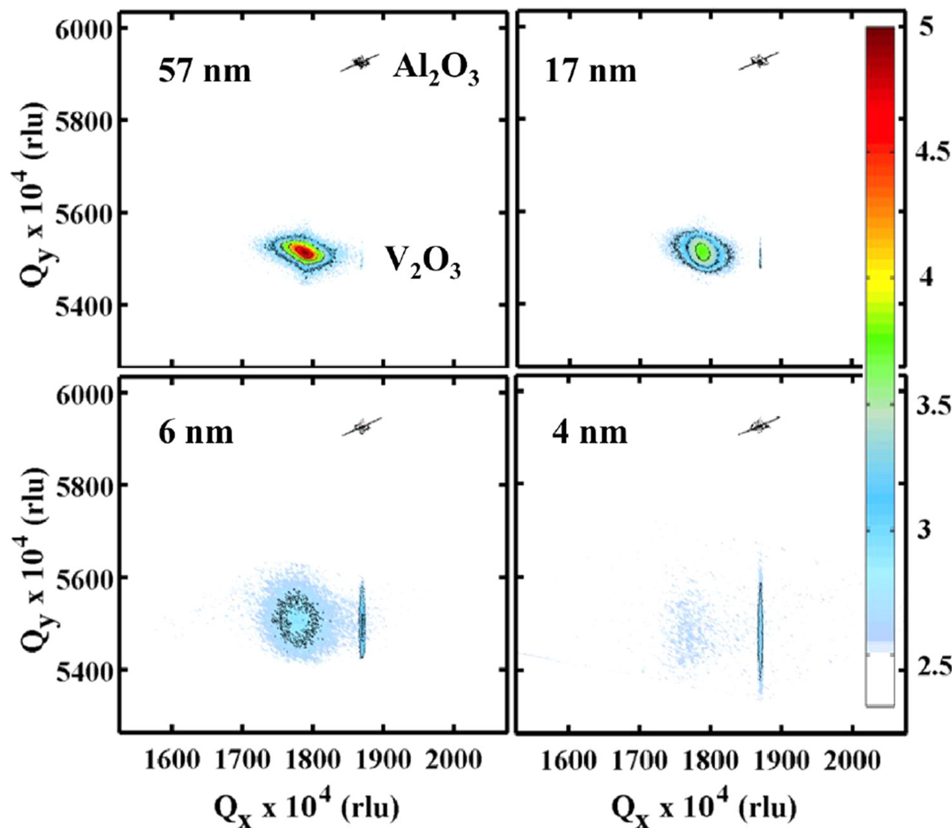

FIG. 2. RSM of the $(1\ 0\ \bar{1}\ 10)$ reflection of V_2O_3 layers deposited directly on (0001)-Al_2O_3. Q_x and Q_y are the components of the scattering vector along in- and out-of-plane directions, respectively. The intensity scale is logarithmic.

heating or cooling curve (whichever is most symmetric) and corrected for the hysteresis. The thickest layer of 73 nm exhibits a MIT of four decades in resistivity at 146 K. The resistivity at room temperature is $1.6 \times 10^{-3}\,\Omega$ cm, slightly higher than the bulk value of about $5 \times 10^{-4}\,\Omega$ cm.[14] As the thickness is decreased to 17 nm, T_{MIT} decreases from 146 K to 131 K and the resistivity ratio (RR), defined as the ratio of resistivity values at 300 K and 120 K, decreases from 7.5×10^4 to 7×10^2.

The layers with thicknesses of 6 and 4 nm exhibit a qualitatively different behavior from the thicker layers. There is no sharp transition and the slope of both cooling and heating curves increases (almost) monotonically with decreasing temperature. There is however still hysteresis present between cooling and heating curves. This suggests that the transition is attenuated significantly in layers that are coherently strained on Al_2O_3. The 4 nm thick sample exhibited a significant asymmetry between measurements along different directions. Whether this is intrinsic, due to sample inhomogeneity or anisotropic crystal sizes needs to be further investigated by conductivity measurements at the nanoscale.

In order to study the possibility of an *intrinsic* critical thickness for the PM-AFI transition to occur, it is necessary to synthesize layers that have a limited interaction with the substrate and bulk-like structural characteristics. For instance, dramatic changes in the transport properties can be directly linked to the epitaxial strain state in ultrathin films of some transition metal oxides.[15] Most of the V_2O_3 thin film work reported in the literature involves the epitaxial deposition of V_2O_3 on substrates that have a rather large misfit with V_2O_3.[3,10–13,16–20] In particular, (0001)-oriented Al_2O_3 with hexagonal unit cell spacings of a = 4.754 Å and c = 12.975 Å is often used as a substrate. Bulk V_2O_3 has lattice spacings of a = 4.954 Å and c = 14.008 Å. The misfit between V_2O_3 and Al_2O_3, defined as $(a_{V203} - a_{Al203})/a_{Al203}$ for deposition on a (0001)-oriented substrate is therefore 4.2%. As a result, below the critical thickness for relaxation via introduction of misfit dislocations, the layer is coherently strained with lattice parameters differing significantly from the bulk values, as can be seen from Fig. 2. Apart from being directly affected by the strain state, the MIT could also be attenuated in coherently strained layers as a result of the strong interaction with the substrate, which could hamper the structural transition to the AFI state. Indeed, it has been shown that enhanced coupling with the (0001)-Al_2O_3 substrate leads to a significant broadening of the V_2O_3 (0006) reflection in XRD and the suppression of the MIT.[16]

In order to lower the substrate influence on thin layers, we have used Cr_2O_3 buffer layers. The misfit between bulk (0001)-V_2O_3 and (0001)-Cr_2O_3 (a = 4.959 Å and c = 13.594 Å) is only −0.1%. We expect therefore a significantly smaller strain for ultrathin V_2O_3 layers deposited on Cr_2O_3. It has already been shown that a buffer layer of Cr_2O_3 significantly decreases the transition width in e-beam evaporated films of 20–450 nm thickness.[21]

RSMs for layers of V_2O_3 grown on a Cr_2O_3 buffer layer are shown in Fig. 4. The thickness of the Cr_2O_3 layers, determined from fits of the XRD data (Fig. 1), is found to vary between 67.5 and 68.5 nm from sample to sample. The thickness of the V_2O_3 layers is determined from XRR. Apart from a faint coherent feature, the Cr_2O_3 is nearly relaxed towards its bulk values, exhibiting a small compressive in-plane strain. Compressive strain is indeed expected from the misfit with the Al_2O_3 substrate. The 56 and 14 nm V_2O_3 layers

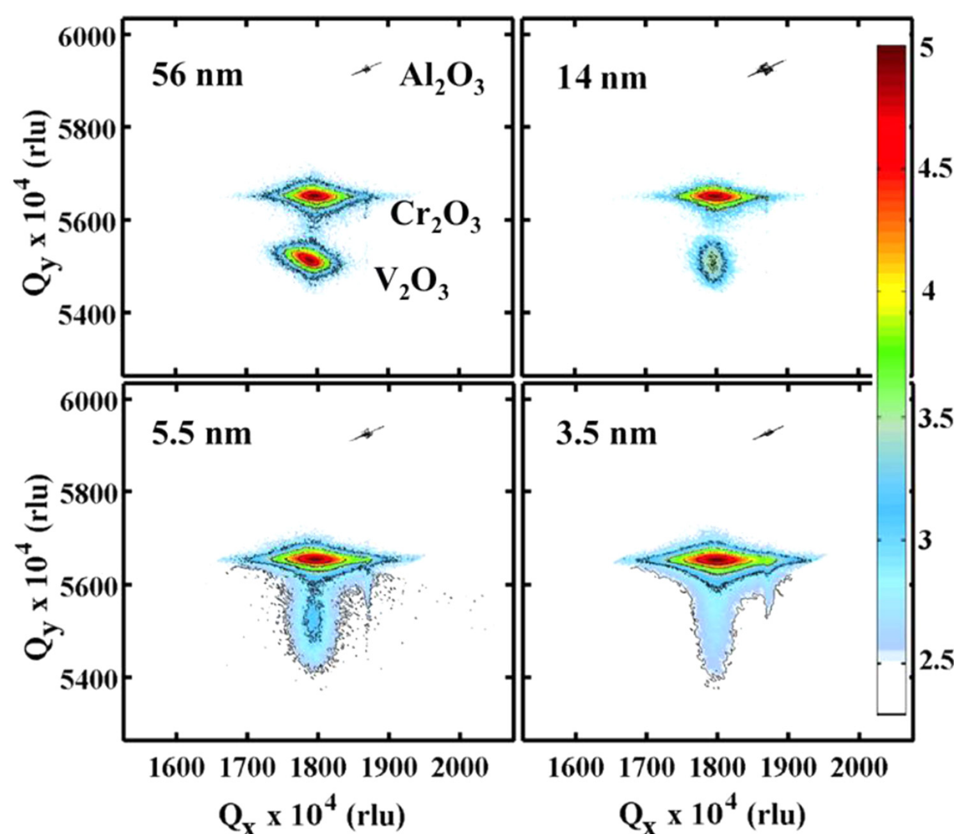

FIG. 4. RSMs of the $(1\ 0\ \bar{1}\ 10)$ reflection of V_2O_3 deposited on Cr_2O_3/(0001)-Al_2O_3. The intensity scale is logarithmic.

exhibit an in-plane (out-of-plane) strain state of 0.21% (−0.47%) and 0.00% (−0.39%), which is possibly thermal in nature. It is clear from the absence of a coherent component (with respect to Al_2O_3) for V_2O_3 as is observed in Fig. 2 that the buffer layer effectively structurally decouples the V_2O_3 layer from the Al_2O_3 substrate.

Fig. 5 shows the resistivity hysteresis curves for V_2O_3 grown on Cr_2O_3/Al_2O_3. We note that Cr_2O_3 is an insulator with a band gap of 3.4 eV and resistivity measurements on independently grown films have shown very high resistivity values. Hence, the features seen in Fig. 5 are entirely to be attributed to those of the thin V_2O_3 layers. The 57 nm layers on Al_2O_3 and 56 nm layer on Cr_2O_3/Al_2O_3 are comparable in terms of hysteresis, transition width and RR (8.1×10^4), but the latter has a higher T_{MIT} around 151 K which is closer to the bulk value. The layers on Cr_2O_3 all exhibit a metallic slope before the MIT with resistivity values between 8.7×10^{-4} and $1.3 \times 10^{-3}\,\Omega$ cm at 300 K. An asymmetry is again sometimes observed between resistances along different directions for the thin layers. In contrast with the thin layers of V_2O_3 deposited directly on Al_2O_3, a MIT is evident in all layers from the sharp increase in resistivity below 150 K and the reduced slope in the insulating region compared to the transition region (notably on the heating curve). From the hysteresis, we find a RR of two orders of magnitude in the 3.5 nm layer.

Coherent strain can have a two-fold effect on the transport properties. On the one hand, the structural transition associated with the MIT can be attenuated due to structural clamping to the substrate. On the other hand, the large strain can dramatically influence the electronic structure. A strain state with respect to bulk V_2O_3 of −4.22 (−4.01)% and +0.09 (−0.17)% for the in- and out-of-plane directions is extracted from the position of the coherent feature of the 4 (6) nm layer shown in Fig. 2. Attempts have been made to associate the strain state in thin V_2O_3 layers with the pressure scale on the bulk phase diagram, based on the a-axis compression[10] and the volume change.[22] Both approaches predict a complete suppression of the MIT and metallic state at all temperatures in our coherent layers. In this context,

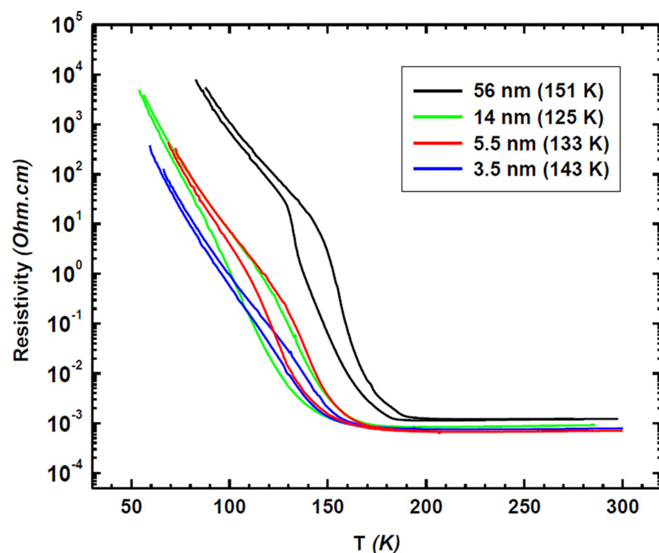

FIG. 5. Resistivity of V_2O_3 layers with different thickness deposited on Cr_2O_3/(0001)-Al_2O_3. T_{MIT} values are given in the legend.

two scenarios can be considered to explain why there is nevertheless still an upturn in resistivity in the 6 and 4 nm layers. First of all, it is possible that the part of the layer, corresponding to the relaxed feature of the 6 and 4 nm samples, does in fact undergo the transition because (as opposed to the coherent part) it is not subject to such large in-plane compressive strain. If this relaxed part is associated with domains that exhibit a wide range of T_{MIT} values, this leads to a coexistence of insulating and metallic domains below the bulk T_{MIT}, where the transport is governed by percolation. On the other hand, the approaches of Refs. 10 and 22 somewhat neglect the role of the strain state along the c-axis, which could be important in determining the electronic state through a dependency of nearest-neighbor distances and trigonal field splitting (closely linked to the MIT[23,24]) on both a-axis and c-axis spacings. In other words, the volume change or a-axis length do not necessarily uniquely determine the state of the system. In this scenario, it is possible that the strain state is not solely responsible for the transport behavior, but clamping can in part cause the attenuation of the MIT.

We expect that the presence of a surface dead layer would, at least in principle, be apparent from an increased resistivity in the metallic phase for a decreasing layer thickness. Our results indicate however a decreased resistivity with decreasing thickness, suggesting that the dead layer should be significantly thinner than 4 nm.

In conclusion, we have significantly changed the in-plane strain state of ultrathin epitaxial V_2O_3 films by about 4.2% using buffer layers of Cr_2O_3 deposited on (0001)-Al_2O_3. Furthermore, we have observed a clear MIT in such V_2O_3 layers as thin as 3.5 ± 1 nm grown on buffer layers of Cr_2O_3. This is in contrast with thin V_2O_3 layers directly grown on Al_2O_3. We explain these results by the different strain state of the V_2O_3 and/or the structural unclamping from the substrate resulting from the insertion of the Cr_2O_3 buffer layer. The demonstration of a MIT in ultrathin layers is of relevance for applications such as piezo-electric and field-effect transistors.

We acknowledge the support from *agentschap voor Innovatie door Wetenschap en Technologie* (IWT) and the *Research Foundation Flanders* (FWO). Discussions with Professor C. Van Haesendonck and Professors M. Van Bael, Bart Ydens, and Petar Bakalov are also acknowledged.

[1] M. Foex, C. R. Acad. Sci. III **223**, 1126 (1946).
[2] D. B. McWhan, J. P. Remeika, T. M. Rice, W. F. Brinkman, J. P. Maita, and A. Menth, Phys. Rev. Lett. **27**, 941 (1971).
[3] H. Schuler, S. Klimm, G. Weissmann, C. Renner, and S. Horn, Thin Solid Films **299**, 119–124 (1997).
[4] S. A. Shivashankar and J. M. Honig, Phys. Rev. B **28**, 5695–5701 (1983).
[5] M. Copel, M. A. Kuroda, M. S. Gordon, X.-H. Liu, S. S. Mahajan, G. J. Martyna, N. Moumen, C. Armstrong, S. M. Rossnagel, T. M. Shaw, P. M. Solomon, T. N. Theis, J. J. Yurkas, Y. Zhu, and D. M. Newns, Nano Lett. **13**(10), 4650–4653 (2013).
[6] Y. Zhou and S. Ramanathan, Crit. Rev. Solid State Mater. Sci. **38**(4), 286–317 (2013).
[7] G. Borghi, M. Fabrizio, and E. Tosatti, Phys. Rev. Lett. **102**, 066806 (2009).
[8] S.-K. Mo, J. D. Denlinger, H.-D. Kim, J.-H. Park, J. W. Allen, A. Sekiyama, A. Yamasaki, K. Kadono, S. Suga, Y. Saitoh, T. Muro, P. Metcalf, G. Keller, K. Held, V. Eyert, V. I. Anisimov, and D. Vollhardt, Phys. Rev. Lett. **90**, 186403 (2003).

[9]F. Rodolakis, B. Mansart, E. Papalazarou, S. Gorovikov, P. Vilmercati, L. Petaccia, A. Goldoni, J. P. Rueff, S. Lupi, P. Metcalf, and M. Marsi, Phys. Rev. Lett. **102**, 066805 (2009).
[10]S. Yonezawa, Y. Muraoka, Y. Ueda, and Z. Hiroi, Solid State Commun. **129**, 245–248 (2004).
[11]C. Grygiel, A. Pautrat, W. C. Sheets, W. Prellier, B. Mercey, and L. Méchin, J. Phys.: Condens. Matter **20**, 472205 (2008).
[12]Q. Luo, Q. Guo, and E. G. Wang, Appl. Phys. Lett. **84**, 2337 (2004).
[13]L. Dillemans, R. R. Lieten, M. Menghini, T. Smets, J. W. Seo, and J. P. Locquet, Thin Solid Films **520**, 4730 (2012).
[14]D. B. McWhan and J. P. Remeika, Phys. Rev. B **2**, 3734–3750 (1970).
[15]J.-P. Locquet, J. Perret, J. Fompeyrine, E. Mächler, J. W. Seo, and G. Van Tendeloo, Nature **394**, 453–456 (1998).
[16]J. Brockman, M. G. Samant, K. P. Roche, and S. S. P. Parkin, Appl. Phys. Lett. **101**, 051606 (2012).
[17]B. S. Allimi, M. Aindow, and S. P. Alpay, Appl. Phys. Lett. **93**, 112109 (2008).
[18]S. Autier-Laurent, B. Mercey, D. Chippaux, P. Limelette, and Ch. Simon, Phys. Rev. B **74**, 195109 (2006).
[19]I. Yamaguchi, T. Manabe, T. Kumagai, W. Kondo, and S. Mizuta, Thin Solid Films **366**, 294–301 (2000).
[20]C. Grygiel, Ch. Simon, B. Mercey, W. Prellier, R. Frésard, and P. Limelette, Appl. Phys. Lett. **91**, 262103 (2007).
[21]H. Schuler, G. Weissmann, C. Renner, S. Six, S. Klimm, F. Simmet, and S. Horn, *Symposium G – Epitaxial Oxide Thin Films II*, edited by D. K. Fork, T. Shiosaki, J. S. Speck, and R. W. Wolf (Mater. Res. Soc. Symp. Proc., 1996), Vol. 401, pp. 61–66.
[22]B. S. Allimi, S. P. Alpay, C. K. Xie, B. O. Wells, J. I. Budnick, and D. M. Pease, Appl. Phys. Lett. **92**, 202105 (2008).
[23]M. S. Laad, L. Craco, and E. Müller-Hartmann, Phys. Rev. Lett. **91**, 156402 (2003).
[24]A. I. Poteryaev, J. M. Tomczak, S. Biermann, A. Georges, A. I. Lichtenstein, A. N. Rubtsov, T. Saha-Dasgupta, and O. K. Andersen, Phys. Rev. B **76**, 085127 (2007).